Extensions of the Cable Equation Incorporating Spatial Dependent Variations in Nerve Cell Diameter

Avis Foster[1], Emily Hendryx[2], Anarina Murillo[3], Michelle Salas[4],
Emmanuel J. Morales-Butler[3],
Sergei Suslov[3], Marco Herrera-Valdez[3]

[1]Department of Mathematical Sciences, George Mason University, Fairfax, VA
[2]Department of Mathematical Sciences, Angelo State University, San Angelo, TX
[3]Mathematical and Computational Modeling Sciences Center, Arizona State University, Tempe, AZ
[4]Department of Biological Sciences, University of Portland, Portland, OR

Abstract

Neuronal function relies on electrical signaling which, in turn, depends greatly on the morphology of neurons. Local changes in the diameter of neurites caused by deformations such as tumors or enlarged cerebral aneurysms may significantly affect electrical conduction. Morphologically accurate models are typically constructed by representing neurons as branched cables, where a system of coupled cable equations represents small neuronal segments as cylinders. Two extensions of the linear cable equation that allow the radius to change continuously in space are constructed here by assuming that the radius of a neuronal segment changes to form a section of a cone or a hyperbolic volume. The cable equation on a cone has an analytical solution involving modified Bessel functions. A more realistic representation of radial deformation is realized by writing the radius as a hyperbolic function of distance along the neurite. The steady state version of the hyperbolic equation is an adapted form of Ince's equation. The cable equation with a hyperbolic radius has an analytical solution only in special conditions, and its numerical solutions can be qualitatively compared to the steady state solutions of the cable equation on a series of cylinders. Unlike the cases for the cylindrical and frustum shapes, the steady state solution of the equation on the hyperbolic cable describes a decay followed by an amplification of voltage along the cable. This counter-intuitive result suggests that non-uniformities in the diameter of neurites have local amplifying effects that may have a non-negligible impact on the propagation of signals in neurons. This research shows how different geometrical representations used to derive cable equations have varying impacts on the calculation of solutions.

1 Introduction

Neurons depend on electrical and chemical signals to transmit information. Abrupt changes in neuronal morphology caused by abnormal growth of neighboring structures might alter its ability to function properly. For example, these structural changes may cause excitations and/or delays in signal transmission that could potentially impact communication at the network level.

The structure and branching of a dendritic tree can strongly influence how synaptic inputs merge to communicate with nearby neurons [6]. Many of the current morphologically accurate models of neurons are constructed by coupling cable equations that represent small neuronal segments as cylinders. The resulting branched cable resembles the original morphology of a neuron, which is used to study the propagation of electrical signals in space and time.

Linear cable equations are typically derived by assuming the membrane acts as an electrical circuit in which resistance and capacitance are arranged in a parallel circuit. The cable equation on a cylinder is derived assuming that charge is conserved using Kirchoff's law and that current flow across the membrane is described by electrical drift (Ohm's law) [10]. The resulting equation is coupled with other equations that represent adjacent portions of a neuron, forming a series of volumetric shapes with varying radii that together may represent whole neurons.

A more geometrically realistic way to model the shape of the neuronal membrane would be to consider radii that are continuous functions of space. The models presented here implement two forms of deformation by assuming different functional forms of the radius in a neuronal segment, respectively, a linear and a hyperbolic function of the distance along a neurite. The cable equation is modified first to incorporate a linear function of the radius, producing a frustum-shaped section of neurite. For the steady-state solution of the frustum, this modification yields a differential equation resembling Lommel's equation and consists of solutions with modified Bessel functions. In the other case, radius is considered to be a hyperbolic function of space, resulting in a steady-state cable equation which takes a form similar to Ince's equation. Comparison of the original cable equation with the modified cable equations that consider space-dependent radii offers insight into voltage propagation through a damaged dendrite.

Modeling possible dendrite deformations as a result of abnormalities is the main interest of this research. This paper proposes three model representations of dendritic branch geometry and investigates the resulting voltage propagation. Studying the effects of a forced dendritic compression indicated that voltage propagation is dependent on the physical properties of dendrites.

2 Methodology

2.1 Mathematical Model

There are several assumptions that must be made prior to investigating the behavior of the voltage and current as they pass through the dendrite. The first assumption is that

any finite part of the dendrite can be represented as a passive, uniform cable with uniform material and electrical properties.

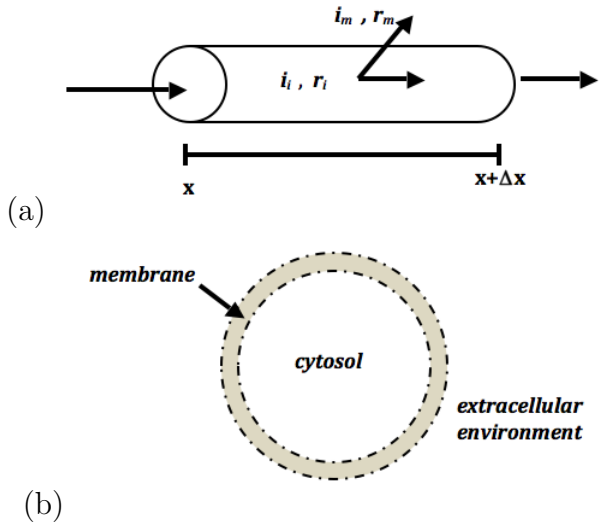

Figure 1: **(a)** Schematic for the dendrite as a cable. Current comes in from the left, and travels a distamce $x+\Delta x$, losing current through the membrane as it travels, but adhering to Kirchoff's current Law. **(b)** A cross-section of a dendritic cable showing the separation between inner and outer parts of the cell.

As shown in Figure 1 (a) current i_i (A) flows through the horizontal axis of the cable and meets a resistance r_i (Ω/cm), calculated by

$$r_i = \frac{R_i}{\pi\left(\frac{d^2}{4}\right)},$$

where R_i (Ωcm) is the specific resistance of the inside of the cable and d (μm) is the cable diameter.

The dendrite membrane separates the inner and outer parts of the cable as shown in Figure 1 (b). The membrane is composed of two regions: sections of resistance and sections of capacitance. Due to the existence of membrane resistance, r_m (Ω/cm), and membrane capacitance, c_m (F/cm), the membrane can be treated as an RC circuit. Here,

$$r_m = \frac{R_m}{\pi d} \text{ and } c_m = C_m \pi d$$

where R_m (Ω cm^2) and C_m (F/cm^2) are the specific resistance and specific capacitance of the membrane, respectively. The capacitance of the membrane causes part of the axial current to flow toward the membrane and out of the dendrite. This membrane current, i_m, "leaks" through the membrane and meets resistance r_m as it leaves the dendrite. Currents i_i and i_m are related through Kirchoff's law of conservation of current,

$$i_{net} = i_i + i_m.$$

The membrane current has a conductive property resulting from r_m and the membrane capacitance. Considering these properties in conjunction with Ohm's law, i_m can be written as

$$i_m = c_m \frac{\partial V}{\partial t} + \frac{V}{r_m}, \tag{1}$$

where V (mV) is the voltage propagated through the cable. Equation (1) and the aforementioned assumptions allow for the derivation of the cable equation,[1]

$$\lambda^2 \frac{\partial^2 V}{\partial x^2} = \tau \frac{\partial V}{\partial t} + V, \tag{2}$$

where $\lambda^2 = \frac{r_m}{r_l}$ is the length constant in centimeters, and $\tau = r_m c_m = R_m C_m$ is the time constant in seconds [10]. General steady state solutions for a cable of finite length (when $\frac{\partial V}{\partial t} \equiv 0$) are of the form,

$$V(X) = V_0 \frac{\cosh(L - X) + B_L \sinh(L - X)}{\cosh(L) + B_L \sinh(L)}, \tag{3}$$

where $X = \frac{x}{\lambda}$ and $L = \frac{l}{\lambda}$ are dimensionless coefficients, and B_L is a constant taken to be a ratio of input conductances [3]. This equation can be modified to describe infinite, semi-infinite, or sealed cables. For the cylindrical segment of dendrite studied in this research, a finite cable is considered. A numerical solution for the finite cable is discussed in the Appendices A, B, and C.

2.2 Cable Equation for a Dendrite of Varying Radius[2]

This section involves spatially dependent radii. Consequently, the cable equation discussed in the previous section is modified so that the radius of the dendrite, r, is now a function of x.

[1] For derivation of the cable equation, see section A in Appendix.

[2] This section is adapted from *Electric Current Flow in Excitable Cells* by JBB Jack, et. al.

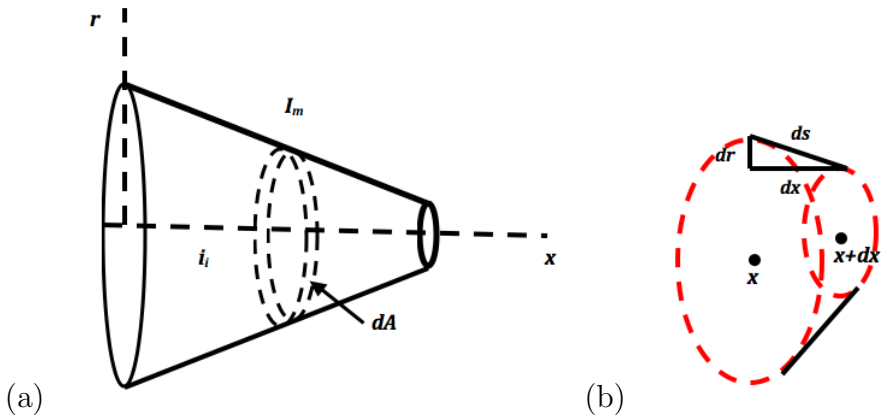

(a) (b)

Figure 2: **(a)** This diagram shows the modified cylinder to allow for changing radius. **(b)** A cross-section of the cylinder with a change in surface area, dA.

From Figure 2 (b), ds (cm) is the change in arc length and dx (cm) is the distance between centers of successive cross-sections of the frustum, Figure 2 (a). The surface area along the cross-section is given by

$$dA = 2\pi r ds, \tag{4}$$

where dA is in units of square centimeters and r is in units of centimeters. The leakage of the interior current over a particular cross-section is given by

$$I_m = -\frac{di_i}{dA}, \tag{5}$$

where I_m (A/cm^2) is the membrane current density[3] and i_i is the axial current. From Figure 2 (b), a right triangle with sides ds, dr, and dx is extracted, and applying the Pythagorean theorem, yields,

$$dx^2 + dr^2 \quad = \quad ds^2$$

which is equivalent to

$$1 + \left(\frac{dr}{dx}\right)^2 \quad = \quad \left(\frac{ds}{dx}\right)^2 \qquad \Rightarrow \qquad \frac{ds}{dx} = \sqrt{1 + \left(\frac{dr}{dx}\right)^2}. \tag{6}$$

Taking the derivative of Equation (4) with respect to x yields an equation for the change in area over the spatial change,

$$\frac{dA}{dx} = 2\pi r \frac{ds}{dx}. \tag{7}$$

[3]The membrane current density is used rather than the membrane current, i_m, since our system no longer has a uniform radius and is thus no longer a homogeneous system [8].

Taking the derivative of Equation (6) with respect to x and rearranging the terms yields.

$$I_m \frac{dA}{dx} = -\frac{\partial i_i}{\partial x}, \tag{8}$$

where the partial derivative of i_i is due to the fact that i_i is a spatial and time dependent function. After applying the assumptions from the original cable equation concerning leakage through the membrane and substituting, $\frac{dA}{dx}$ in Equation (7) into Equation (8), the following series of equations are derived,

$$I_m \left(2\pi r \frac{ds}{dx}\right) = -\frac{\partial i_i}{\partial x}, \tag{9}$$

$$I_m = \frac{V}{R_m} + C_m \frac{\partial V}{\partial t}, \tag{10}$$

$$i_i = -\frac{\pi r^2}{R_i} \frac{\partial V}{\partial x}. \tag{11}$$

The derivative of Equation (11) with respect to x gives

$$\frac{\partial i_i}{\partial x} = -\frac{2\pi r}{R_i} \frac{\partial V}{\partial x} \frac{dr}{dx} - \frac{\pi r^2}{R_i} \frac{\partial^2 V}{\partial x^2}. \tag{12}$$

Substituting the preceding equation for $\frac{\partial i_i}{\partial x}$ into Equation (9),

$$I_m 2\pi r \frac{ds}{dx} = \frac{2\pi r}{R_i} \frac{\partial V}{\partial x} \frac{dr}{dx} + \frac{\pi r^2}{R_i} \frac{\partial^2 V}{\partial x^2} \quad \Rightarrow \quad I_m \frac{ds}{dx} = \frac{1}{R_i} \frac{\partial V}{\partial x} \frac{dr}{dx} + \frac{r}{2R_i} \frac{\partial^2 V}{\partial x^2}. \tag{13}$$

Applying Equation (10) to Equation (13) yields,

$$\left(\frac{V}{R_m} + C_m \frac{\partial V}{\partial t}\right) \frac{ds}{dx} = \frac{1}{R_i} \frac{\partial V}{\partial x} \frac{dr}{dx} + \frac{r}{2R_i} \frac{\partial^2 V}{\partial x^2}. \tag{14}$$

Equation (14) is multiplied by R_m leading to

$$\left(V + C_m R_m \frac{\partial V}{\partial t}\right) \frac{ds}{dx} = \frac{R_m}{R_i} \frac{\partial V}{\partial x} \frac{dr}{dx} + \frac{r R_m}{2R_i} \frac{\partial^2 V}{\partial x^2} \tag{15}$$

$$\Rightarrow \left(V + \tau \frac{\partial V}{\partial t}\right) \frac{ds}{dx} = \frac{R_m}{R_i} \frac{\partial V}{\partial x} \frac{dr}{dx} + \frac{r R_m}{2R_i} \frac{\partial^2 V}{\partial x^2}. \tag{16}$$

The left-hand side of Equation (16) becomes the time dependent component of the original cable equation multiplied by a rate of change in arc length along the frustum, $\frac{ds}{dx}$; the right-hand side of Equation (16) represents the voltage's dependency on space. Thus, the modified cable equation is obtained, allowing different functions for the radius to be inserted and the results of voltage propagation to be examined through a deformed dendrite.

2.3 Using Lommel's Equation for Conical Cable Equation

In this section, the case of a linearly changing radius is investigated, that is, a slice of the frustum is isolated as shown below.

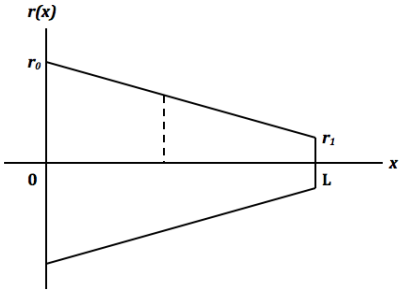

Figure 3: A cross-section of the frustum.

From the diagram, the equation of the line connecting the points (0, r_0) and (L, r_1) is

$$r = r_0 + \frac{r_1 - r_0}{L}x, \qquad r(0) = r_0, \qquad r(L) = r_1, \tag{17}$$

and therefore the slope of the equation satisfies

$$\frac{dr}{dx} = \frac{r_1 - r_0}{L}, \tag{18}$$

which is then substituted into equation (6) to obtain

$$\frac{ds}{dx} = \sqrt{1 + \left(\frac{r_1 - r_0}{L}\right)^2}, \tag{19}$$

which is a constant.
The original cable equation is used to find an expression for $\frac{\partial^2 V}{\partial x^2}$ with respect to the linear radius. The derivative of the voltage with respect to x is

$$\frac{\partial V}{\partial x} = \frac{r_1 - r_0}{L}\frac{\partial V}{\partial r}. \tag{20}$$

Using Equation (20), and assuming voltage is a well-behaved function implies that

$$\frac{\partial^2 V}{\partial x^2} = \left(\frac{r_1 - r_0}{L}\right)^2 \frac{\partial^2 V}{\partial r^2}. \tag{21}$$

Combining Equations (20) and (21) gives

$$\left(V + \tau\frac{\partial V}{\partial t}\right)\sqrt{1 + \left(\frac{dr}{dx}\right)^2} = \frac{R_m}{R_i}\left(\frac{r_1 - r_0}{L}\right)^2 \frac{\partial V}{\partial r} + \frac{rR_m}{2R_i}\left(\frac{r_1 - r_0}{L}\right)^2 \frac{\partial^2 V}{\partial r^2}. \tag{22}$$

By setting $\frac{\partial V}{\partial t} = 0$ and multiplying the above equation by $\frac{2r_i}{rR_m}\left(\frac{L}{r_1-r_0}\right)^2$, rearrangement of terms yields

$$\frac{d^2V}{dr^2} + \frac{2}{r}\frac{dV}{dr} - \frac{1}{r}\frac{2R_i}{R_m}\frac{\sqrt{1+\left(\frac{r_1-r_0}{L}\right)^2}}{\left(\frac{r_1-r_0}{L}\right)^2}V = 0, \tag{23}$$

which is a special form of a Lommel's equation,

$$V'' + \frac{1-2\alpha}{\xi}V' + \left[\left(\beta\gamma\xi^{\gamma-1}\right)^2 + \frac{\alpha^2-\nu^2\gamma^2}{\xi^2}\right]V = 0, \tag{24}$$

with solution

$$V(\xi) = \xi^2 u_\nu(\beta\xi^\gamma) \tag{25}$$

Equation (23) is a special case of Lommel's Equation (24) where,

$$\xi = r, \quad \alpha = -\frac{1}{2}, \quad \gamma = \frac{1}{2}, \quad \nu = \pm 1, \quad \beta^2 = -\frac{8R_i}{R_m}\frac{\sqrt{1+\left(\frac{r_1-r_0}{L}\right)^2}}{\left(\frac{r_1-r_0}{L}\right)^2}.$$

Lommel's equation has solutions with modified Bessel functions since β has imaginary parts. The linearly independent solutions are

$$V_1 = \frac{1}{\sqrt{r}}I_1\left(\sqrt{\frac{8rR_i\sqrt{1+(\frac{r_1-r_0}{L})^2}}{R_m(\frac{r_1-r_0}{L})^2}}\right), \tag{26}$$

$$V_2 = \frac{1}{\sqrt{r}}K_1\left(\sqrt{\frac{8rR_i\sqrt{1+(\frac{r_1-r_0}{L})^2}}{R_m(\frac{r_1-r_0}{L})^2}}\right), \tag{27}$$

where I_1 and K_1 are modified Bessel functions. The general solution of Equation (23) is therefore

$$V = C_1V_1 + C_2V_2. \tag{28}$$

Coefficients of the general solution are determined by the boundary conditions, which are discussed in the following section.

2.4 Boundary Conditions for Linearly Defined Radius

For the case of a cone, the conical steady state solution is given by

$$r\frac{d^2V}{dr^2} + 2\frac{dV}{dr} = \frac{2R_i}{R_m}\left(\frac{\sqrt{1+\left(\frac{r_1-r_0}{L}\right)^2}}{\left(\frac{r_1-r_0}{L}\right)^2}\right)V, \tag{29}$$

with radius:

$$\begin{aligned} r &= r(x), \\ r(x) &= r_0 + \frac{r_1 - r_0}{L}x, \qquad 0 \le x \le L. \end{aligned}$$

A steady state solution in the form of modified Bessel functions is

$$V(x) = V_0\left(\frac{C_1(L-X) + B_L S_1(L-X)}{C_1(L) + B_L S_1(L)}\right), \tag{30}$$

with the boundary conditions:

$$V(0) = V_0, \qquad B_L V(L) + \frac{dV}{dx}(L) = 0.$$

This is obtained by applying initial conditions:

$$S_1 = 0, \qquad S_1'(0) = 1, \qquad C_1(0) = 1, \qquad C_1'(0) = 0.$$

C_1 and S_1 are composed of V_1, V_2, and constants involving modified Bessel functions:

$$S_1(x) = \frac{2Lr_0^{3/2}}{(r_1 - r_0)\sqrt{r}}\left(K_1(\beta\sqrt{r_0})I_1(\beta\sqrt{r}) - I_1(\beta\sqrt{r_0})K_1(\beta\sqrt{r})\right), \tag{31}$$

$$\begin{aligned} C_1(x) &= (\beta\sqrt{r_0}K_0(\beta\sqrt{r_0}) + 2K_1(\beta\sqrt{r_0})))\sqrt{\frac{r_0}{r}}I_1(\beta\sqrt{r}) \\ &+ (C\sqrt{r_0}I_0(\beta\sqrt{r_0}) - 2I_1(\beta\sqrt{r_0}) - 2I_1(\beta\sqrt{r_0}))\sqrt{\frac{r_0}{r}}K_1(\beta\sqrt{r}), \end{aligned} \tag{32}$$

where

$$\beta = \sqrt{\frac{8R_i}{R_m}}\left(\frac{(1+(\frac{r_1-r_0}{L})^2)^{1/4}}{\frac{r_1-r_0}{L}}\right).$$

Thus, the final steady state equation is obtained,

$$r\frac{d^2V}{dr^2} + 2\frac{dV}{dr} = \frac{\beta^2}{4}V \tag{33}$$

These boundary conditions yield a steady state solution, allowing for analysis of voltage propagation through a sealed frustum.

2.5 Hyperbolic Functions

An alternate formulation of how the aneurysm or tumor constricts the dendrite employs a hyperbolic function to represent how the radius depends on x:

$$r(x) = a\cosh\left(\frac{x}{a}\right) + b, \tag{34}$$

where a (cm) represents the shape of the abnormality and b represents how much the dendrite is compressed in units of centimeters. In order to find an expression for b, the two known points $r(0) = a + d$ and $r(a) = \frac{d}{2}$ are used:

$$\begin{aligned} r(a) &= a\cosh(1) + b \\ &= \frac{d}{2}, \\ r(0) &= a\cosh(0) + b \\ &= a + b. \end{aligned}$$

Thus,

$$b = r(0) - a.$$

Substituting this value of b into $r(a)$ leads to

$$r(a) = \frac{d}{2} = acosh(1) + r(0) - a \quad \Rightarrow \quad \frac{d}{2} = a(\cosh(1) - 1) + r(0)$$

which can be solved for $r(0)$ to obtain b,

$$r(0) = \frac{d}{2} - a(\cosh(1) - 1) \quad \Rightarrow \quad b = \frac{d}{2} - a\cosh(1). \tag{35}$$

Since $a\cosh\left(\frac{x}{a}\right) \geq 1$ and the shift in hyperbolic cosine cannot be greater than the radius itself, it is clear that $-1 \leq b \leq \frac{d}{2} - 1$.

After taking the derivative of r in Equation (34) with respect to x and substituting it into Equation (6) gives the following results,

$$\frac{ds}{dx} = \sqrt{1 + \sinh\left(\frac{x}{a}\right)} = \sqrt{\cosh^2\left(\frac{x}{a}\right)} \quad \Rightarrow \quad \frac{ds}{dx} = \cosh\left(\frac{x}{a}\right).$$

Applying Equation (15) yields,

$$\left(V + C_m R_m \frac{\partial V}{\partial t}\right)\cosh\left(\frac{x}{a}\right) = \frac{R_m}{R_i}\sinh\left(\frac{x}{a}\right)\frac{\partial V}{\partial x} + \frac{R_m}{2R_i} r \frac{\partial^2 V}{\partial x^2} \tag{36}$$

For the steady state solution of the hyperbolic, the following is obtained,

$$\begin{aligned} V\left(\cosh\left(\frac{x}{a}\right)\right) &= \frac{R_m}{2R_i}\left(2\sinh\left(\frac{x}{a}\right)\frac{dV}{dx} + \left(a\cosh\left(\frac{x}{a}\right)+b\right)\frac{d^2V}{dx^2}\right) \\ \Rightarrow V\frac{2R_i}{R_m}\left(\cosh\left(\frac{x}{a}\right)\right) &= 2\sinh\left(\frac{x}{a}\right)\frac{dV}{dx} + \left(a\cosh\left(\frac{x}{a}\right)+b\right)\frac{d^2V}{dx^2}. \end{aligned}$$

$$\begin{aligned} \left(b + a\cosh\left(\frac{x}{a}\right)\right)\frac{d^2V}{dx^2} + 2\sinh\left(\frac{x}{a}\right)\frac{dV}{dx} - \frac{2R_i}{R_m}\left(\cosh\left(\frac{x}{a}\right)\right)V &= 0 \\ \Rightarrow \left(1 + \frac{a}{b}\cosh\left(\frac{x}{a}\right)\right)\frac{d^2V}{dx^2} + \frac{2}{b}\sinh\left(\frac{x}{a}\right)\frac{dV}{dx} - \frac{2R_i}{bR_m}\left(\cosh\left(\frac{x}{a}\right)\right)V &= 0, \end{aligned} \quad (37)$$

where $b \neq 0$. Here, the equation takes a form similar to that of Ince's equation, which is

$$(1 + a_0\cos(2s))y'' + b_0\sin(2s)y' + (c_0 + d_0\cos(2s))y = 0, \quad (38)$$

where a_0, b_0, c_0, and d_0 are arbitrary constants. Ince's equation is used to study the existence of periodic solutions, in several applications in mathematical physics To study the modified cable equation with a hyperbolic radius, Equation (38) is taken to have imaginary arguments, since β is complex, and becomes

$$(1 + a_0\cosh(2s))y'' + b_0\sinh(2s)y' + (c_0 + d_0\cosh(2s))y = 0. \quad (39)$$

The presented modified form of Ince's equation is not known to have been studied prior to this research. To study a space-dependent radius, a change of variables is used to rewrite Equation (39) as,

$$\left(1 + a_0\cosh\left(\frac{x}{a}\right)\right)y'' + b_0\sinh\left(\frac{x}{a}\right)y' + \left(c_0 + d_0\cosh\left(\frac{x}{a}\right)\right)y = 0. \quad (40)$$

To put Equation (37) in the form of Equation (40), coefficients of Equation (40) are defined as

$$\begin{aligned} a_0 &= \frac{a}{b} \\ b_0 &= \frac{2}{b} \\ c_0 &= 0 \\ d_0 &= -\frac{2R_i}{bR_m}. \end{aligned}$$

Equation (40) will be studied numerically and compared with the numerical solutions of the other equations for the deformed dendrite.

3 Results: Steady State Solutions

In order to investigate the voltage propagation through a series of dendritic segments, the cylinder, hyperbolic, and frustum shapes are combined as shown in Figure 4.

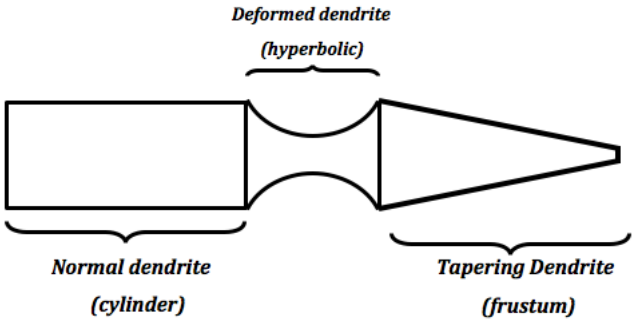

Figure 4: Series of different dendrite radius types

Each shape is first studied individually before the system is examined as a whole. Recall the steady state solution for the cylindrical cable given Equation (3). For the purposes of this project, only one specific set of parameters is considered: $R_i = 50$ cm, $R_m = 10^3$ Ωcm^2, $V_0 = -50$ mV, d $= 5$ μm, $B_L = 0.5$, and $l = 20$ μm. In all graphs, the vertical axis is shifted such that the membrane resting potential of -65 mV is represented at y $= 0$. Thus, 15 mV on the vertical axis is actually -50 mV. Figure 5 displays the voltage through a cylinder.

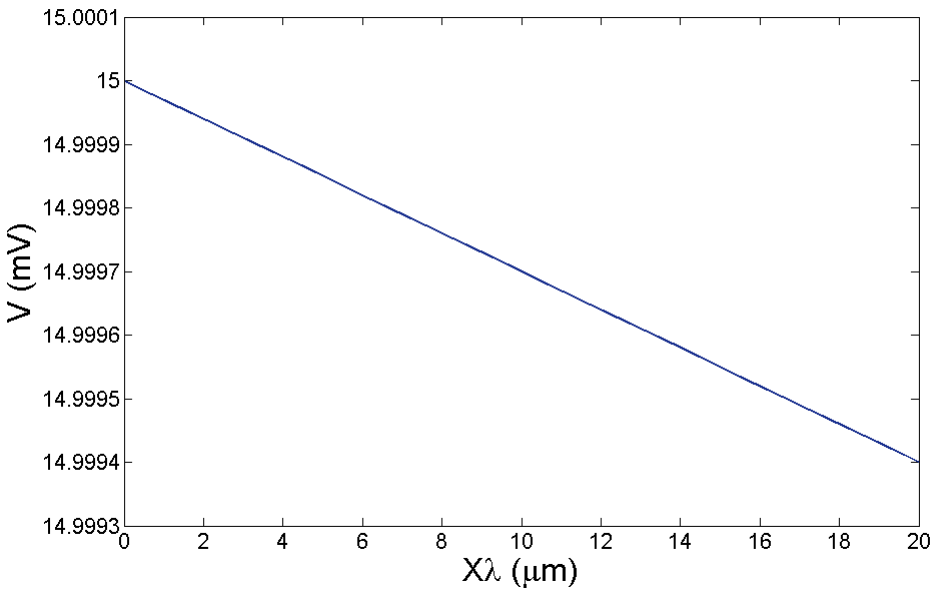

Figure 5: Steady State Voltage for Cylinder with Respect to Space: $V_0 = 15$ mV, d = 5 μm, $B_L = 0.5$, and $l = 20$ μm.

Though the change in voltage seems to be linear in Figure 5, it is important to note that the solution involves functions of L and X, where $L = l/\lambda$ and $X = x/\lambda$ - two small, dimensionless numbers. The graph appears linear because it is a small segment of the hyperbolic curve that results from the solution for a finite cylindrical cable. The shown decay in voltage is expected due to the fact that voltages typically tend toward resting membrane potential. Note that the voltage drop is in the scale of microvolts.

For convenience in combining the segments, the next case considered is a radius that is a hyperbolic function of x; the initial voltage and initial $\frac{dV}{dx}$ are taken to be the same as the final voltage of the cylindrical case: $V_0 \approx 14.9994$ and $\frac{dV}{dx} \approx -2.9999 \cdot 10^{-5}$ $\frac{V}{\mu m}$. The initial diameter, R_i, and R_m are also taken to be the same values given for a uniform radius, and $a = 1\mu$m. Because there are no known analytical solutions for the modified Ince's equation, the results for this case rest almost entirely on numerical solutions of the system.

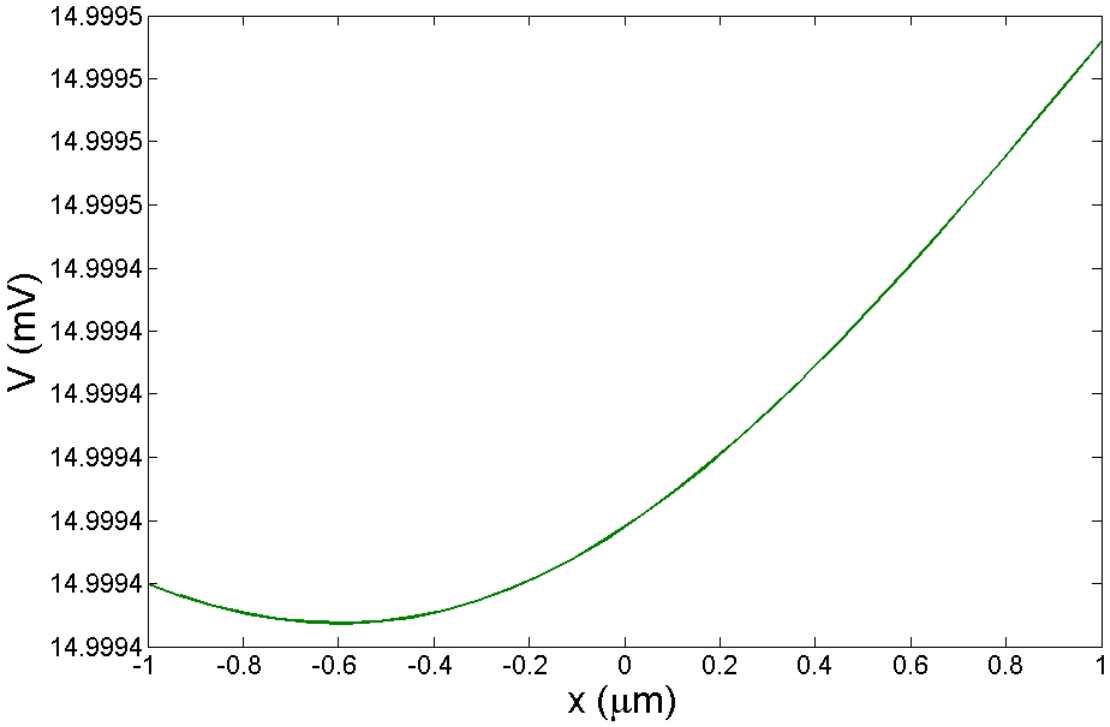

Figure 6: Steady state voltage for hyperbolic with respect to space: $d = 5\mu$m, $V_0 \approx 14.9994$ $\frac{dV}{dx} \approx -2.9999 \cdot 10^{-5}$ $\frac{V}{\mu m}$, and $a = 1$.

As shown in Figure 6, the voltage first decreases as a result of the initial $\frac{dV}{dx}$ and then increases in an exponential manner. The reason for this apparent amplification in voltage, though quite small, is unclear and calls for further study.

To verify that the result for the hyperbolic radius is mathematically sound, consider the case where $b = 0$. In this instance, the modified cable equation strays from Ince's equation and can be written as:

$$\begin{aligned}
\left(0 + a\cosh\left(\frac{x}{a}\right)\right)\frac{d^2V}{dx^2} + 2\sinh\left(\frac{x}{a}\right)\frac{dV}{dx} - \frac{2R_i}{R_m}\left(\cosh\left(\frac{x}{a}\right)\right)V &= 0 \\
\Rightarrow \left(a\cosh\left(\frac{x}{a}\right)\right)\frac{d^2V}{dx^2} + 2\sinh\left(\frac{x}{a}\right)\frac{dV}{dx} &= \frac{2R_i}{R_m}\left(\cosh\left(\frac{x}{a}\right)\right)V \\
\Rightarrow \frac{d^2V}{dx^2} + 2\frac{\sinh\left(\frac{x}{a}\right)}{a\cosh\left(\frac{x}{a}\right)}dV\,dx &= \frac{2R_i}{R_m}\frac{\cosh\left(\frac{x}{a}\right)}{\cosh\left(\frac{x}{a}\right)}V \\
\Rightarrow \frac{d^2V}{dx^2} + \frac{2}{a}\tanh\left(\frac{x}{a}\right)dV\,dx &= \frac{2R_i}{R_m a}V
\end{aligned}$$

This equation can be compared to

$$\frac{d^2y}{dx^2} + 2\lambda\tanh(\lambda x)\frac{dy}{dx} = \mu_0^2 y,$$

which has the known solution:

$$y = \frac{C_1 \sinh(\mu x) + C_2 \cosh(\mu x)}{\cosh(\lambda x)},$$

where $\mu = \sqrt{(\mu_0^2 + \lambda^2)}$ and C_1 and C_2 are arbitrary constants. Letting $\lambda = \frac{1}{a}$ and $\mu_0 = \frac{2R_i}{aR_m}$, the solution to the hyperbolic case when $b = 0$ is

$$V = \frac{C_1 \sinh\left(\frac{x}{a}\sqrt{\left(\frac{2R_i}{R_m}\right)^2 + 1}\right) + C_2 \cosh\left(\frac{x}{a}\sqrt{\left(\frac{2R_i}{R_m}\right)^2 + 1}\right)}{\cosh\left(\frac{x}{a}\right)}$$

Comparison between the analytical and numerical solutions when $b = 0$ is shows that the numerical solution qualitatively agrees with the analytical solution.

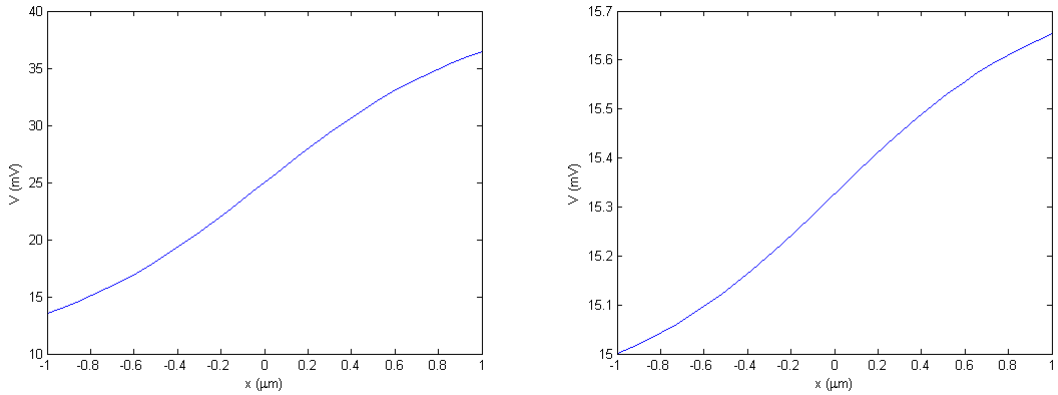

Figure 7: **Left:** Analytical Solution. **Right:** Numerical Solution. Comparing these two graphs shows that the two solutions take the same qualitative form. Differences in scale and slope are most likely due to the arbitrary constants and derivatives chosen.

The last situation considered is the case for a radius that is a linear function of x. Again, the parameters are the same as previously defined for the cylinder aside from the initial voltage. This initial voltage for the frustum is the final voltage of the hyperbolic case and thus, $V_0 \approx 14.9995$ mV. Using the general solution for a finite cylinder, setting $B_L = 0$ in equation (3) gives the solution

$$V(X) = V_0 \frac{C_1(L - X)}{C_1(L)},$$

for the function C_1 given in Section 2.4. In this case, the values of L and X are simply taken to be x and l. From the numerics used to reach this solution involving Bessel functions, Figure 8 shows that voltage decreases in a seemingly exponential manner as the radius of the frustum decreases.

This voltage drop is relatively large in comparison to the voltage changes of the other

two cases, but it is still a drop of less than 0.1 mV. Not only does voltage usually decrease along a uniform dendrite, but the initial value conditions for this problem also allow for decreasing voltage in frustums of both increasing and decreasing diameters. Thus, this graphical result seems reasonable.

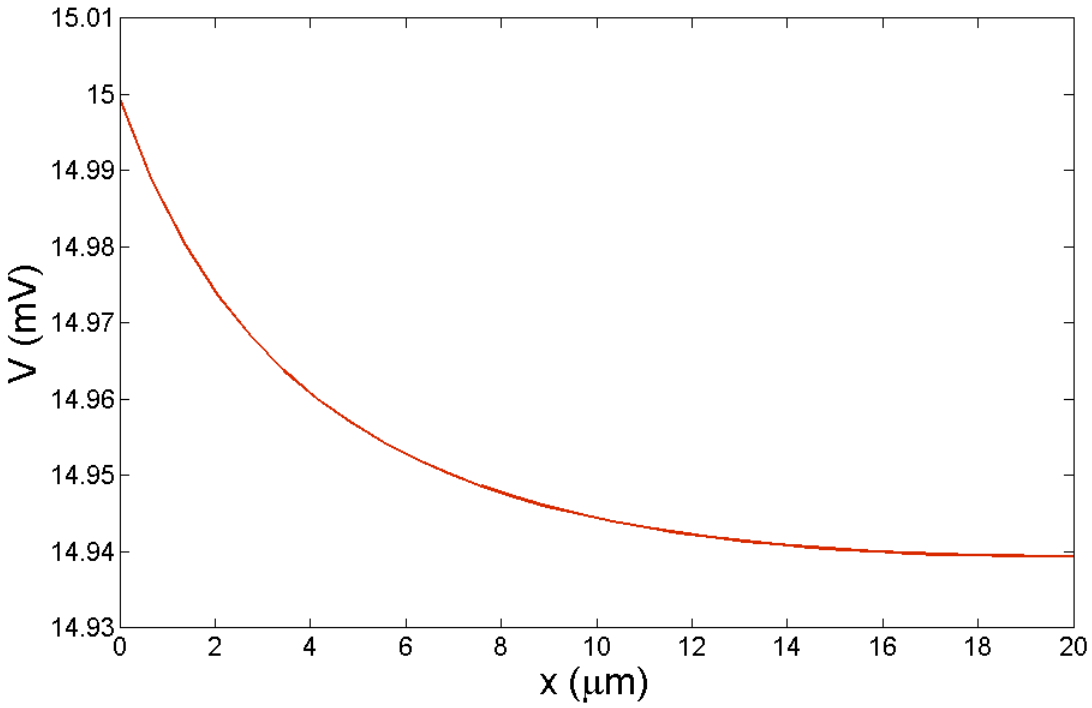

Figure 8: Steady State Voltage for Cone with Respect to Space: $V_0 \approx 14.9995$ mV, $r_0 = 2.5\mu$m, $r_1 = 0.5\mu$m, and $l = 20$ μm.

The results for the three cases discussed above allow for the investigation of a system in which the cylinder, hyperbolic radius, and frustum are combined in series. This is due to the fact that the voltage and $\frac{dV}{dt}$ are assumed to be maintained at each junction. Because this condition is met for the circumstance presented throughout the section, the parameters previously stated are applicable. Thus, the structural situation shown in Figure 4 is considered: the system containing a uniform radius, a radius that is a hyperbolic function of x, and a radius that is a linear function of x.

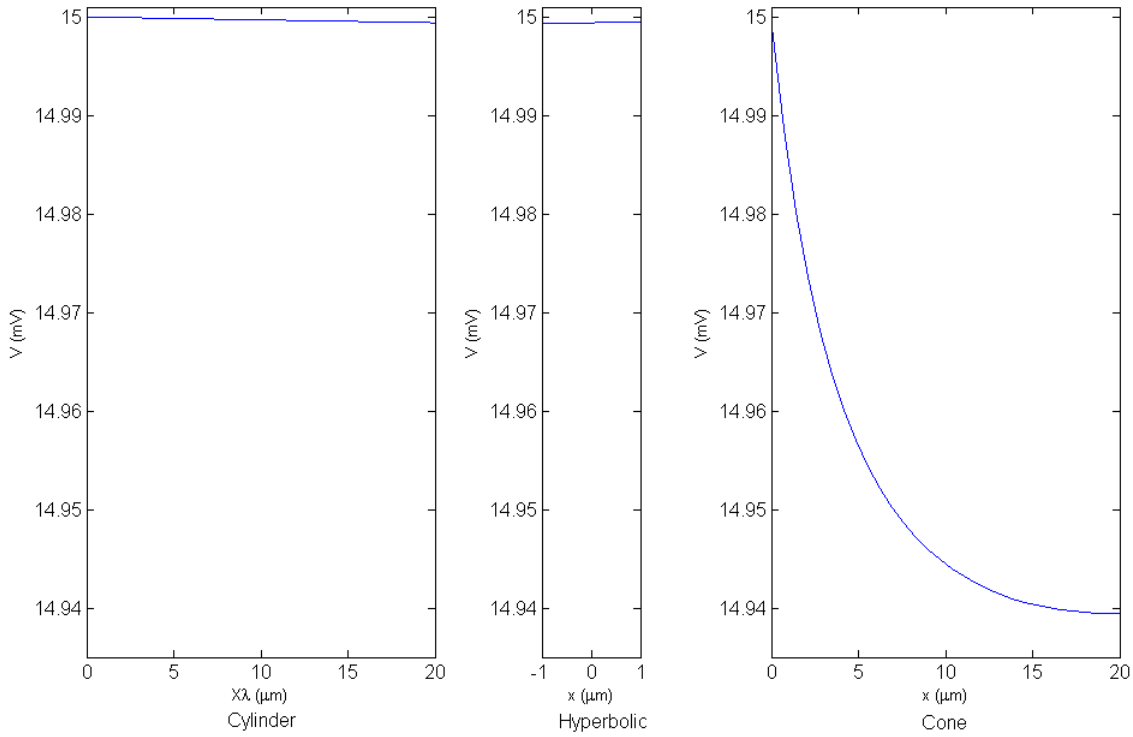

Figure 9: Each respective plot represents the voltage behavior in each of the three regions as shown in Figure 4 (Note: The horizontal axis is not set to the same scale for each graph)

By arranging the graphs in the shape of a possible dendrite deformation, the voltage propagation throughout the dendrite segment as a whole becomes more clear (see Figure 5). The solution for a cylinder of the same length as the combined segments is presented for the sake of comparison between a non-deformed dendrite and one of varying diameters.

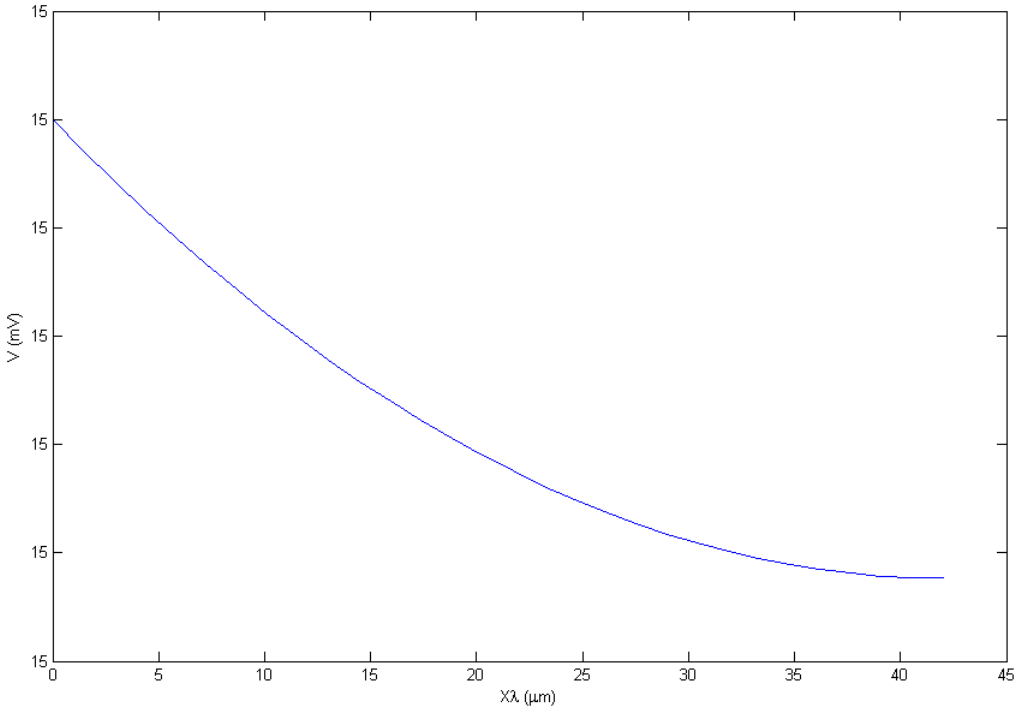

Figure 10: Steady state of a cylinder without deformation.

3.1 Discussion

In studying the changes in voltage throughout neurites, the overall decrease in voltage over x were expected. The results for the cylinder were consistent with biological and mathematical findings. Though the drop in voltage from the cone was expected, the rate of decrease was higher than predicted and requires further investigation. In the case of the hyperbolic radius, the solutions were inconsistent with widely accepted biological models using series of cylinders. Typically, as spatially-dependent diameter decreases and increases in a manner similar to the hyperbolic curve, the voltage drops toward the membrane resting potential. As seen in Figure (6), the use of a radius that is a hyperbolic function of x does not accurately produce this same result of decreasing voltage. Though Figure 7 shows that the numerical method used is in fact mathematically correct, the biological aspects are not realistic. Thus, the hyperbolic radius offers an interesting mathematical approach to modelling dendritic deformation but does not appear to have any biological relevance.

4 Conclusions and Future Work

Structures exerting abnormal pressure on neurons, such as a tumor or aneurysm, influence dendritic morphology of a single nerve cell. Cerebral aneurysms are present in

almost 5% of Americans, and more than 600,000 Americans have been diagnosed with brain tumors [1]. Results from this research could have applications in determining how aneurysms or tumors could affect voltage propagation, which could lead to greater insight into neuronal function in adverse environments. It can be inferred through examining change in voltage as consequence

In this project, the neuronal model considered three cases where the radius behaved differently, either held constant or was spatially dependent. Assuming a formation already exists, the cable equation was modified to represent two additional geometric forms of deformation. Although, the model presented offers insight into dendritic deformation and how it could affect voltage propagation, limitations prevent a comprehensive understanding of neuronal function in adverse conditions.

One way to improve the model would be to consider the presence of ion channels along the dendritic membrane and see how the transfer of potassium, sodium, calcium, and chloride is affected by the impeding growth. These ions contribute to the regulation of voltage, and examining them may result in a deeper understanding of biological implications. Since the model focused on a single dendritic branch, another possible expansion could include the entire dendritic tree. This would allow for generalizations about how the entire neuron functions in the presence of abnormal growths. Though only one hyperbolic function was used in this model, other hyperbolic functions may be explored in future work especially since they may not be in the form of a modified Ince's equation. Due to the time constraints of this summer project, we only considered one set of parameters. In the future, changing these parameters to account for variation in size or shape of the anomaly would give greater insight into how growths in the brain affect neuronal function.

5 Acknowledgements

Foremost, we would like to thank Carlos Castillo-Chavez, Executive Director of the Mathematical and Theoretical Biological Institute, for giving us the opportunity to participate in this research program. A special thanks is also given to our mentors Aprillya Lanz, Jose Vega, and Karen Rios-Soto, MTBI Summer Director, for all their insight and support. This project has been supported by grants from the National Science Foundation (NSF - Grant DMPS-0838705), the National Security Agency (NSA - Grant H98230-09-1-0104), the Alfred P. Sloan Foundation; and the President and Provost Offices at Arizona State University. The Mathematical and Theoretical Biology Institute now hosted at the Mathematical, Computational and Modeling Science Center at ASU would like to give thanks to everybody involved with the program for the past 15 years.

References

[1] American Brain Tumor Association. *http://www.abta.org* July 23, 2010.

[2] V. Comincioloi, , D. Funaro, A. Torelli, E. D'Angelo, , and P. Rossi, A Mathematical Model of Potential Spreading Along Neuron Dendrites of Cerebellar Granule Cells, *Applied Mathematics and Computation, 59*(1), (1993) 73-87.

[3] Comp Neuroscience, *Passive cell Models.* Retrieved at http://www.physics.nmt.edu/ rsonnenf/phys321/matlabDifferential%20Equations% 20in% 20MATLAB.pdf (1998)

[4] M. DiStasio, *Numerical Solutions to the Passive Cable Equation: Using Finite Difference Approximations to Partial Derivatives.* SUNY Downstate Medical Center and NYU-Poly (2010).

[5] I. Dvorak and A. Holden, *Mathematical approaches to brain functioning diagnostics.* Proceedings in nonlinear science. Manchester University Press, Manchester; UK.

[6] A. T. Gulledge, B. M. Kampa, G. J. Stuart, *Synaptic Integration in Dendritic Trees.* Division of Neuroscience, John Curtin School of Medical Research, The Australian National University, Canberra, ACT 0200, Australia (2004).

[7] E. M. Izhikevich, *Dynamical systems in neuroscience.* MIT Press. Cambridge; Massachusetts. (2007)

[8] JJB. Jack, D¿ Noble, and RW. Tsien, *Electric current flow in excitable cells.* Oxford; UK. (1983)

[9] J. Keener and J. Sneyd, *Mathematical Physiology.* Springer, New York; NY. (2008)

[10] C. Koch and I. Segev, *Methods in Neuronal Modeling: From Synapses to Networks.* MIT Press. Cambridge; Massachusetts. (1989)

[11] M. Kroon and G. A. Holzapfel, A model for saccular cerebral aneurysm growth by collagen fibre remodeling. *Journal of Theoretical Biology, 247*(4), (2007) 775-787.

[12] M. London and I. Segev, Conducting synaptic music in dendrites. *Nature Neuroscience, 7*(9), (2004) 904-905.

[13] M. London and M. Hausser, Dendritic Computation. *Annual Review Neuroscience, 28*:(2005) 503-532.

[14] T. J. Sejnowski and K. M. Stiefel, Mapping Function Onto Neuronal Morphology. *Journal of Neurophysiology, 98*(1) (2007) 513-526.

[15] H. Tuckwell, *Introduction to theoretical neurobiology: volume 1: linear cable theory and dendritic structure.* Cambridge University Press, New York; NY (1988).

[16] H. Tuckwell, *Introduction to theoretical neurobiology: volume 2: nonlinear and stochastic theories.* Cambridge University Press, NewYork; NY. (1988)

[17] J. Wood, *Cerebral Blood Flow.* McGraw-Hill Book Publishing Company. New York; NY. (1987)

Appendix

A Derivation of the Cable Equation

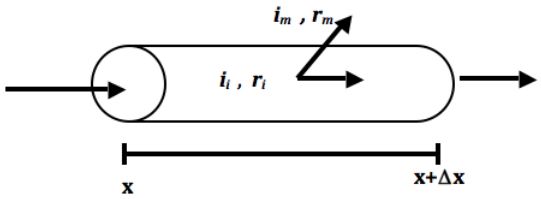

Starting with Ohm's law, consider a change in potential as the current I_{in} moves from x to $x + \Delta x$, where

$$V_i(x + \Delta x) - V_i(x) = -i_i(x) r_i \Delta x, \tag{41}$$

for a specific time, since V_i is in terms of space and time. The right-hand side is negative because as the current moves form the left to right sides of the cable, there is some leakage through the membrane that cause the axial current to be less than it was coming in. Then divide by Δx and take the limit of both sides. Since r_i is only dependent on the diameter of the cable ($r_i = \frac{R_i}{\pi(\frac{d^2}{4})}$), it can be considered a constant.

$$\frac{\partial V_i}{\partial x} = -i_i r_i. \tag{42}$$

A relationship between the interior current and the current that is being leaked through the membrane is made since there is a drop in the interior current over space as the membrane current increases. Therefore,

$$\begin{aligned} i_m &= -\frac{\Delta i}{\Delta x}, \\ i_m &= -\frac{\partial i_i}{\partial x}. \end{aligned} \tag{43}$$

Since there exists a relationship between the membrane current and the current through the neurite. Equation (2) is used to find a relationship between the voltage and the

membrane current through the second derivative with respect to x.

$$\begin{aligned}
\frac{\partial^2 V}{\partial x^2} &= -r_i \frac{\partial i_i}{\partial x}, \\
\frac{\partial^2 V}{\partial x^2} &= r_i(-\frac{\partial i_i}{\partial x}), \\
\frac{\partial^2 V}{\partial x^2} &= r_i i_m, \\
\frac{1}{r_i}\frac{\partial^2 V}{\partial x^2} &= i_m.
\end{aligned} \tag{44}$$

Then it is stated that $V = V_i - V_e - E_r$ and also the extracellular voltage, V_e, is not dependent on x or t. Further, it is also said that the battery, E_r, is independent of x and t. Thus, V_i is changed to V in equation (4). So far, only the voltage of the intracellular region was considered and now the inner and outer voltages are combined into one equation. Then r_m ($\frac{R_m}{\pi d}$), the actual membrane resistance, is multiplied and the right-hand side is the membrane voltage, V_m.

$$\frac{r_m}{r_i}\frac{\partial^2 V_i}{\partial x^2} = i_m r_m.$$

One assumption is that the membrane acts as a capacitor that holds charge, and this relationship between charge, voltage and capacitance is used to find an expression for i_m in terms of the capacitance, c_m (constant = $C_m \pi d$),

$$\begin{aligned}
Q &= c_m V, \\
\frac{\partial Q}{\partial t} &= c_m \frac{\partial V}{\partial t},
\end{aligned} \tag{45}$$

and also in terms of the current that actually comes across the membrane from the intercellular current. This is done by applying Kirchoff's current law.

$$i_m = c_m \frac{\partial V}{\partial t} + \frac{V}{r_m},$$

By multiplying r_m to the previous equation the following is obtained,

$$r_m i_m = c_m r_m \frac{\partial V}{\partial t} + V, \tag{46}$$

then the value $c_m r_m$ is the time constant τ,which reduces to the material properties of the membrane, and is therefore independent of the diameter.

$$\tau = r_m c_m = \frac{R_m}{\pi d} C_m \pi d = R_m C_m.$$

Afterwards, substituting i_m from equation (4) yields the cable equation.

$$\begin{aligned} r_m i_m &= \tau \frac{\partial V}{\partial t} + V, \\ \frac{r_m}{r_i} \frac{\partial^2 V}{\partial x^2} &= \tau \frac{\partial V}{\partial t} + V, \\ \lambda^2 \frac{\partial^2 V}{\partial x^2} &= \tau \frac{\partial V}{\partial t} + V. \end{aligned} \tag{47}$$

The term $\lambda = \sqrt{\frac{r_m}{r_i}}$ is defined as the length constant, which depends on the diameter of the cylinder.

B Units Table

Notation	Definition	Units
i_i	Intracellular current	A
i_m	Membrane current	A
I_m	Membrane current density	$\frac{A}{cm^2}$
r_i	Intracellular resistance	$\frac{\Omega}{cm}$
r_m	Membrane resistance	$\Omega \cdot cm$
R_i	Specific intracellular resistance	$\Omega \cdot cm$
R_m	Specific intracellular resistance	$\Omega \cdot cm^2$
c_m	Membrane capacitance	$\frac{F}{cm}$
C_m	Specific membrane capacitance	$\frac{F}{cm^2}$
τ	Time constant	s
λ	Length constant	cm
dA	Change in area of the cross-section	cm^2
ds	Change in arc length	cm